Computational Fluid Dynamics Analysis of the Offending Artery at Sites of Neurovascular Compression in Trigeminal Neuralgia Using Preoperative MRI Data

Kenji YAMADA,[1] Yoji TANAKA,[1] Kazutaka SUMITA,[2]
Shigeru NEMOTO,[2] and Taketoshi MAEHARA[1]

[1]Department of Neurosurgery, Tokyo Medical and Dental University, Tokyo, Japan;
[2]Department of Endovascular Surgery, Tokyo Medical and Dental University, Tokyo, Japan

Abstract

This study aimed to analyze the hemodynamic features of the offending artery at sites of neurovascular compression (NVC) using computational fluid dynamics (CFD). A total of 23 patients who underwent microvascular decompression (MVD) for primary trigeminal neuralgia (TN) between January 2015 and December 2016 were enrolled in this study. The compressing vessel at the NVC site was identified microsurgically in all cases, and patients were divided into two groups based on the intraoperative findings: (1) the arterial NVC group and (2) the non-arterial NVC control group. A 3D surface model of the structures surrounding the NVC was created using preoperative magnetic resonance imaging (MRI), and CFD analysis was performed for the target artery. In addition to standard parameters, such as the wall shear stress (WSS), flow velocity, and pressure, we calculated the WSS ratio (WSSR) by dividing the WSS at the NVC by the mean WSS of the target. Arterial compression was observed intraoperatively in 13 patients. The mean WSSR of the arterial NVC group was significantly higher than that of the control group (2.36 ± 1.00 vs. 1.18 ± 0.73, $P < 0.05$). There were no significant intergroup differences in the other calculated parameters. High WSSR, which indicates elevated WSS at the sites of NVC, was identified as a unique parameter of arterial compression that may contribute to TN. CFD could be a useful clinical tool in determining the target of MVD under preoperative conditions.

Key words: trigeminal neuralgia, computational fluid dynamics, wall shear stress, offending artery, microvascular decompression

Introduction

Neurovascular compression (NVC) at the trigeminal root entry zone is widely considered to be the main cause of trigeminal neuralgia (TN), and microvascular decompression (MVD) has been shown to provide effective symptomatic relief by releasing the vascular compression.[1–5] However, the neurophysiological mechanism underlying TN still remains unclear. As NVC involves vascular compression to the nerve, and arterial compression is more likely to be symptomatic, the hemodynamic forces acting on the vessel wall at the NVC site may contribute to the pathogenesis of TN. A previous report revealed focal axonopathy and demyelination at the site of indentation of the

trigeminal nerve in patients with TN.[6] Therefore, monitoring the focal hemodynamic forces of the offending artery could increase our understanding of the mechanisms underlying TN.

As NVC is the target of MVD, demonstration of the clear anatomical structure of NVC by magnetic resonance imaging (MRI) studies provides important information for preoperative assessment. Whereas information obtained in MRI demonstrates the position or relation of the trigeminal nerve with compressing vessels in most cases, there are some cases when MRI cannot identify the offending artery, including cases where the artery passes through the nearby trigeminal nerve without obvious contact or in cases that involve multiple vessel contacts with the trigeminal nerve. Moreover, NVC is also observed in many asymptomatic patients. Therefore, an objective parameter to differentiate symptomatic compressions from incidental findings could have implications for surgical decision-making and prognosis of MVD.

Computational fluid dynamics (CFD) is a numerical analysis method used to solve problems involving fluid flow. Recent advances in medical imaging and CFD have made it possible to simulate blood flow patterns in anatomically realistic models. Many studies have used CFD to analyze the hemodynamic characteristics in cerebral vascular disorders, such as atherosclerosis and intracranial aneurysms, and indicated particular parameters that are related to the cause of the disease.[7–13]

This study aimed to develop a 3D surface model of the offending artery based on the patient's preoperative MRI image and analyze the hemodynamic features using CFD. Specific parameters related to symptomatic compressions were searched.

Materials and Methods

Patient population

This retrospective study was approved by the Ethics Committee at Tokyo Medical and Dental University, Tokyo, Japan. Patients who underwent MVD at the Institute from January 2015 to December 2016 were enrolled in the study. The enrollment criteria was as below: (1) patients diagnosed with primary TN according to the *International Classification of Headache Disorders*,[14] (2) patients who had compressing vessels that were identified microsurgically, and (3) patients with high-resolution MRI datasets. All surgical procedures were performed via a retrosigmoid suboccipital approach. Compressing vessels were defined as vessels that contacted and formed indentations with the nerve directly and transposed from the conflicting site. When several compressing vessels were found during the operation, only the main compressing vessel was considered. According to the intraoperative findings, patients were divided into the arterial NVC and non-arterial NVC control groups.

Imaging and modeling

All enrolled patients underwent 3T MRI imaging (GE Signa HDxt, GE Healthcare, Waukesha, WI, USA), including 3D fast imaging employing steady-state acquisition (FIESTA) scans, before surgery. The sequence parameters were as follows: repetition time (TR), 8.7 ms; echo time (TE), 2.7 ms; flip angle, 70°; field of view, 230 mm; matrix, 512; slice thickness, 0.6 mm. All MRI images were transferred to commercial software Avizo (version 6.3.0, FEI, Portland, OR, USA) for preprocessing. Structures surrounding the NVC, including the arteries, veins, trigeminal nerve, and brainstem, were segmented to each object, and 3D surface models were created (Fig. 1). The irregularities resulting from slice gaps

were refined using an isotropic 3D Gaussian smoothing filter. In the arterial NVC group, the surface model showed obvious contact of an offending artery with the trigeminal nerve. The contacting point on the artery surface was defined as the NVC site; contact of an artery was not always obvious in the non-arterial NVC control group. For such cases, the artery with the shortest distance between the artery surface and the trigeminal nerve surface was identified as the analysis artery, and the point of the artery with minimal distance to the trigeminal nerve was defined as the NVC site. Surface models of the offending artery were trimmed out for CFD analysis. The computational meshes, with mesh sizes between 0.5 and 1 million elements, were generated for these artery models.

Numerical simulations

Wall shear stress (WSS), one of the distinctive parameters obtained from CFD simulation, expresses the force per unit area exerted by the wall on the fluid in a direction on the local tangent plane. We applied CFD to the artery models using the solver function of commercial software SCRYU/TETRA V9 (Software Cradle, Osaka, Japan). The CFD theory was adapted and modified from previous reports.[15–17] In brief, blood was assumed as an incompressible Newtonian fluid with a density of 1050 kg/m^3 and a viscosity of 0.004 N/m^2/s. Vessel walls were assumed to be rigid with no slip conditions. A straight inlet extension was added to obtain a completely developed laminar flow. For the inlet condition, fixed mass flow, which yields a WSS of 2 N/m^2 at the inlet, was used. Traction-free boundary conditions were applied at the outlets. A steady-state analysis was performed and the target region, which was a 20 mm long portion of the offending artery with the NVC at the center, was extracted for post-processing. The average WSS and pressure of the target region were calculated. The average WSS of the tiny spot with a diameter of 0.1 mm around the NVC was defined as the WSS at the NVC. The average flow velocity of the cross-section of the artery at the NVC was defined as the flow velocity at the NVC. As the magnitude of WSS differs depending on the vessel's anatomical structure, we calculated the WSS ratio (WSSR) by dividing the WSS at the NVC by the average WSS of the target region.

Statistical analysis

All statistical analyses were performed with JMP statistical software (version 13.2, SAS Institute Inc., Cary, NC, USA). The Mann–Whitney U test was used to identify differences between the two groups (arterial NVC and non-arterial NVC control groups). Data was presented as mean ± standard
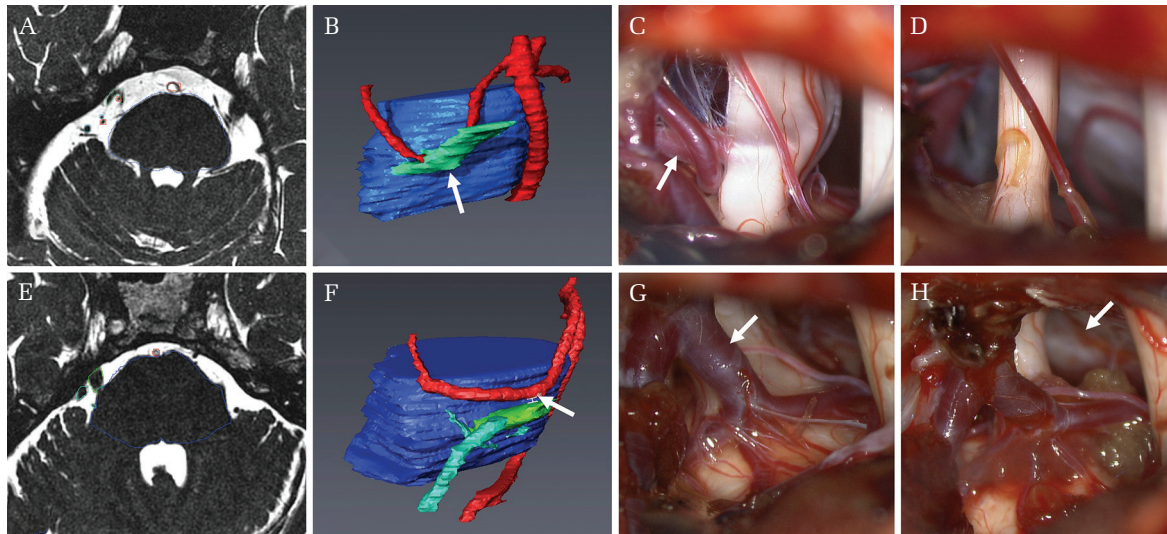
Fig. 1 Representative examples of the modeling process. (A–D) Representative case of arterial neurovascular compression (NVC). The patient is a 70-year-old male with right-sided trigeminal neuralgia (TN). (A) Segmentation of arteries (*red*), trigeminal nerve (*green*), and brainstem (*blue*) was performed based on the fast imaging employing steady-state acquisition (FIESTA) image. (B) The 3D surface model. Compression of the superior cerebellar artery (SCA) is demonstrated. The white arrow indicates the NVC site. (C) Intraoperative photograph of the right trigeminal nerve revealing the compression by the SCA (*white arrow*). (D) Postoperative photograph. The SCA is transposed away from the nerve. (E–H) Representative case of non-arterial NVC. The patient is a 65-year-old woman with right-sided TN. (E) The segmented objects are the arteries (*red*), trigeminal nerve (*green*), brainstem (*blue*), and veins (*light blue*). (F) The 3D surface model demonstrates compression of a vein. The *white arrow* indicates the nearest point on the SCA from the trigeminal nerve, which is defined as the NVC site in this non-arterial NVC case. (G) Intraoperative photograph revealing compression by a vein (*white arrow*) and its branches. (H) Postoperative photograph revealing interposition of pieces of oxidized cellulose between the nerve and the vein. The *white arrow* indicates the SCA, which is the analyzed vessel of this case, running behind the trigeminal nerve.

deviation (SD), and a probability value (*P*) <0.05 was considered statistically significant.

Results

Patient characteristics

Among the 31 patients who underwent MVD during the study period, a total of 23 patients were enrolled in the study. A total of eight patients were excluded for the following reasons: high-resolution MRI datasets were unavailable (*n* = 3), could not identify the compressing vessel microsurgically (*n* = 5). Patient characteristics are summarized in Table 1. Arterial compression was observed intra-operatively in 13 patients. The superior cerebellar artery (SCA) and anterior inferior cerebellar artery (AICA) was responsible for arterial compression in 10 and three patients, respectively. In the non-arterial compression group (*n* = 10), the transverse pontine vein was identified as the compressing vessel in all cases. In the non-arterial NVC control group, SCA and AICA were analyzed as the nearby artery in eight and two patients, respectively. A complete CFD analysis was carried out for all patients.

Table 1 Patient characteristics

Variables	NVC group	Non-arterial NVC control group
Mean age (years)	64.5 ± 12.7	56.6 ± 15.1
Gender		
Men	8	1
Women	5	9
Side		
Right	11	8
Left	2	2
Compressing vessels		
SCA	10	
AICA	3	
TPV		10
Analyzed (nearby) artery		
SCA	10	8
AICA	3	2

AICA: anterior inferior cerebellar artery, NVC: neurovascular compression, SCA: superior cerebellar artery, TPV: transverse pontine vein.

Presentation in representative cases

Two representative examples of the process for creating 3D surface models are shown in Fig. 1. One is a case of arterial compression (Figs. 1A–D) and the other is a case of non-arterial compression (Figs. 1E–H), which were confirmed intraoperatively. The NVC site was also determined and presented on the created surface model preoperatively (Figs. 1B and 1F). Visualization of the calculated hemodynamic features of a representative arterial compression case is shown in Fig. 2. Elevation of WSS at the NVC site was demonstrated qualitatively on the color map. There were no specific findings for the distribution of the other parameters.

Values of the calculated parameters

The calculated mean values for all cases were as follows: WSS at the NVC site was 5.54 ± 7.32 N/m², which was higher than the average WSS of the target
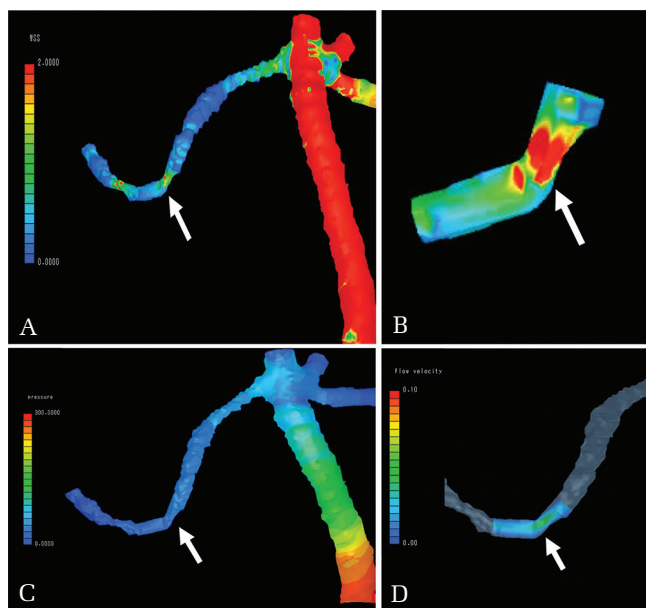

Fig. 2   Visualization of the hemodynamics of a representative case with an arterial neurovascular compression (NVC). (A) The distribution of wall shear stress (WSS) is shown in 3D geometry. The unit of the color bar is N/m². *White arrows* indicate the NVC site. (B) WSS distribution of the extracted target region. Elevation of WSS is recognized at the NVC site (*white arrow*). The magnitude of WSS at the NVC site is 1.47 N/m², and the average WSS of the target region is 0.37 N/m². (C) The distribution of pressure. The unit of the color bar is N/m². The magnitude of pressure depends on the distance from the inlet, but there are little differences around the target region. The average pressure of the target region is 29.8 N/m². (D) The flow velocity field is shown in the cross-sectional plane of the target region. The unit of the color bar is m/s. The average flow velocity is 0.041 m/s.

region 3.12 ± 4.01 N/m²; this difference was not statistically significant. The average WSS value differed in each case by three orders of magnitude in linkage with the average flow velocity, which was 0.21 ± 0.25 m/s. The mean WSSR was 1.85 ± 1.04. Unlike the absolute value of WSS, the WSSR ranged from 0.31 to 3.70, which was comparable among individual cases. The average pressure at the artery region was 163 ± 254 N/m².

Comparisons of each parameter between the arterial NVC and the non-arterial control groups

Comparisons of each parameter, including WSS at the NVC site, flow velocity, average pressure at the target region, and the WSSR, between the arterial NVC and the non-arterial groups are shown in Fig. 3. The mean WSSR of the arterial NVC group was significantly higher than that of the control NVC group (2.36 ± 1.00 vs. 1.18 ± 0.73, $P <0.05$). No significant intergroup differences were observed for the other calculated parameters. The mean values for each group are as follows (arterial NVC vs. non-arterial NVC control): WSS at the NVC site: 7.20 ± 8.45 N/m² vs. 3.37 ± 5.70 N/m², $P = 0.067$; average WSS at the target region: 3.20 ± 3.99 N/m² vs. 3.02 ± 4.56 N/m², $P = 0.598$; average pressure at the target region: 173.0 ± 314.8 N/m² vs. 149.5 ± 179.4 N/m², $P = 0.877$; and flow velocity: 0.205 ± 0.202 m/s vs. 0.203 ± 0.320 m/s, $P = 0.336$.

Impact of the tortuosity of the analyzed artery

To examine the impact of vessel tortuosity in WSSR elevation, cases with tortuous vessels were excluded for further analysis. Curvature at the NVC site with an angle more than 30° was defined tortuous. About seven tortuous vessels in the arterial NVC group and four in the non-arterial NVC group were excluded and a total of 12 cases (six cases from each group) were analyzed. The mean WSSR of each group were 2.27 ± 0.96 vs. 1.18 ± 0.91 ($P = 0.093$). The mean WSSR of the arterial NVC group was higher than the non-arterial group, though the difference was not statistically significant.

Discussion

Microvascular decompression has been the standard treatment for TN since it was introduced by Jannetta.[2] As the aim of MVD is to transpose the compressing blood vessel and relieve the trigeminal nerve compression, identification of NVC, which is the target of MVD, is important in preoperative assessment. MRI is used widely as the main modality to detect NVC; in particular, fusion images of 3D FIESTA and 3D time-of-flight magnetic resonance
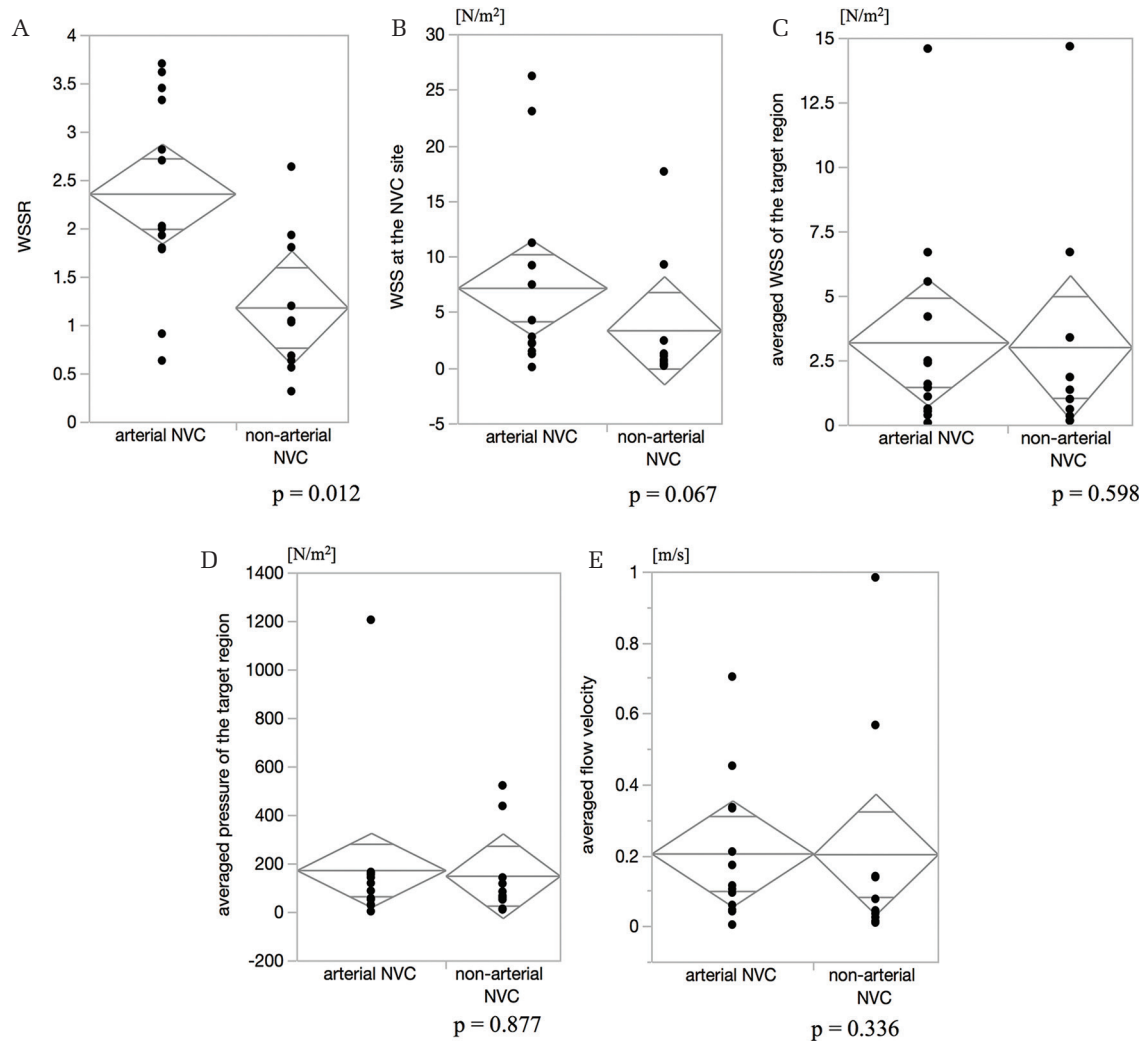
Fig. 3 Comparisons of each parameter between the arterial and non-arterial neurovascular compression (NVC) groups. The dot plots of the calculated values of the two groups (arterial NVC and non-arterial NVC) are shown. The horizontal line indicates the mean value and the diamond extends from the lower to the upper confidence limit. (A) The wall shear stress ratio (WSSR) of the arterial NVC group was significantly higher than that of the non-arterial group, $P < 0.05$. (B) The mean WSS at the NVC site of the arterial NVC group was slightly higher than that in the non-arterial group, but this difference was not statistically significant. (C–E) There were no significant differences between the two groups in (C) average WSS of the target region, (D) average pressure, and (E) average flow velocity.

angiography using 3T MRI scanners are reported to be efficient tools for visualizing and assessing vascular compression.[18,19]

Although NVC has been precisely revealed by these high-resolution preoperative images, this approach only provides information regarding the anatomical contact of the vessel and nerve. However, assessment of the pathogenicity of the compression is necessary to explore the cause of TN because NVC also occurs in many asymptomatic patients.[4] Antonini et al.[20] reported that patients with NVC at the caudal root exit zone, which is the proximal portion of the trigeminal nerve, are more likely to be symptomatic. Herweh et al.[21] studied severe TN

patients using diffusion tensor imaging (DTI) and found that the loss of anisotropy detected by DTI indicates tissue damage of the trigeminal nerve. Lin et al.[22] reported that a large diameter of the compressing artery increases the chances of the contact being symptomatic. These studies assessed the morphological features of the NVC, which is static information. Since arteries are more likely to become symptomatic than veins, dynamic information, like flow, velocity, or pressure derived from blood flow, would also affect the pathogenicity of NVC.

Since the assessment of local hemodynamic parameters of cerebral arteries *in vivo* is difficult, image-based CFD simulations have recently been

proposed to investigate the local hemodynamics of cerebral vascular diseases, especially cerebral aneurysms. Among the various parameters obtained from CFD simulation, WSS has been considered to play a key role in the interaction between blood flow and surrounding tissue. WSS is a frictional force of the blood on the epithelial layer and is known to modulate intracellular signaling cascades and gene expression via stimulation of mechanoreceptors on the endothelial cells, resulting in the formation of cerebral vascular diseases, such as cerebral aneurysm and atherosclerosis.[23,24]

Thus, WSS may be used to indicate hemodynamic stress caused by the blood flow of the offending artery in TN patients, and there may be a relationship between WSS and the pathogenicity of NVC. In our cases, the magnitude of WSS differed depending on anatomical factors, such as the artery diameter, branches around the target region, tortuosity of the artery, and the distance from the basilar artery. Because of this dispersion of WSS, it was necessary to use the WSSR, which was calculated by dividing the WSS at the NVC site by the average WSS of the target region, to perform statistical analysis of the calculated data.

Recent studies have indicated the involvement of CFD in neurovascular compression syndrome.[25–27] Satoh et al.[26] retrospectively analyzed the offending artery of 20 symptomatic TN and hemifacial spasm patients and reported a relatively high magnitude of WSS and restriction of WSS directional movement along the NVC compared with the surrounding site of NVC. According to this study, a high WSSR, which indicates focal elevation of WSS at the NVC site, has the potential to identify symptomatic compressions.

Based on intraoperative findings, patients in the current study were divided into two groups, the arterial NVC and non-arterial NVC groups. Among patients in the non-arterial group, there were cases where arterial NVC was depicted in the preoperative MRI images; however, the pathogenicity was difficult to judge only from the MRI images. We observed a significantly higher WSSR in the arterial NVC group than in the non-arterial NVC control group, which suggests that WSSR may be a useful indicator for evaluating ambiguous NVCs. In particular, in cases with several involving vessels, information regarding the pathogenicity would be useful for preoperative simulation of MVD. The elevation of WSSR could be attributable to the strong compression of the symptomatic arterial NVC causing conformational changes in both the trigeminal nerve and compressing artery. These conformational changes are extremely small and difficult to detect intuitively from preoperative images; however, hemodynamic values obtained from CFD are highly sensitive and are able to identify these small changes. In addition, the obtained parameters are numerical values that can be analyzed both intuitively and statistically.

Although WSS is a hemodynamic force acting on the arterial wall, the elevated WSS at the NVC site may affect the trigeminal nerve. This may cause degeneration because of the tight contact between the arterial wall and nerve. This phenomenon may provide clues for understanding the occurrence of TN.

Nevertheless, this study had some limitations. The analyzed artery model had some geometric uncertainty, and the rightness of the boundary conditions was unclear. Although the targets of this study were relatively small arteries with diameters of 1–2 mm, we adapted the methodology of CFD for analysis of cerebral aneurysms whose targets are larger arteries with diameters of 2–5 mm. CFD analysis for cerebral aneurysms, especially small branches occurring from large parent arteries, results in little blood flow and pressure, which could be ignored. Validation and verification of the CFD analysis for such small arteries are required.

Anatomical features of the vessel which could affect the WSS value should be assessed to clarify the mechanism of the WSSR elevation in the arterial NVC group. In regard to vessel tortuosity, cases without tortuous curvature at the NVC site were extracted for additional analysis. WSSR was higher in the arterial NVC group, which suggest the contribution of the arterial compression, but the difference was not statistically significant. As the sample size is small, further study is required.

To evaluate the performance of CFD analysis as a clinical test to discern ambiguous NVCs, consideration should be limited to patients who have arterial contact detected on MRI images. An appropriate cut-off value of WSSR should be defined based on receiver operating characteristic analysis, and the sensitivity and specificity should be evaluated.

Another limitation is that the focal axonal degeneration and demyelination of the trigeminal nerve, which are the causes of TN, are not considered in this study. The correlation between the microstructural changes in the trigeminal nerve revealed by DTI and the hemodynamic stress of the offending artery should be investigated in future studies. Furthermore, the small patient population and the retrospective nature of the study did not allow us to draw a precise conclusion on the effects of hemodynamic stress in TN. A prospective study with a larger number of patients is essential for further discussion.

However, unlike recent CFD studies using computed tomography angiogram for the construction of artery

models,[25–27)] the CFD technique used in this study is based on non-contrast-enhanced preoperative MRI, which is a simple and completely non-invasive method that provides useful information about the pathogenicity of NVC. This CFD technique should be considered during preoperative simulation of MVD.

Conclusion

We demonstrated the hemodynamic features of the offending artery using a CFD technique. Focal elevation of WSS at the site of the NVC, which suggests symptomatic arterial compression, was identified as a unique parameter that could be the reasons for TN. The CFD technique could be a useful clinical tool for determining the target of MVD under preoperative conditions.

Acknowledgments

Conflicts of Interest Disclosure

The authors report no conflicts of interest concerning the materials or methods used in this study or the findings specified in this paper. All authors who are members of the Japan Neurosurgical Society (JNS) have registered online, self-reported COI Disclosure Statement forms through the website for JNS members.

References

1) Barker FG, Janneta PJ, Bissonette DJ, Larkins MV, Jho HD: The long-term outcome of microvascular decompression for trigeminal neuralgia. *N Engl J Med* 334: 1077–1083, 1996

2) Jannetta PJ: Arterial compression of the trigeminal nerve at the pons in patients with trigeminal neuralgia. *J Neurosurg* 26: 159–162, 1967

3) Meaney JF, Eldridge PR, Dunn LT, Nixon TE, Whitehouse GH, Miles JB: Demonstration of neurovascular compression in trigeminal neuralgia with magnetic resonance imaging. Comparison with surgical findings in 52 consecutive operative cases. *J Neurosurg* 83: 799–805, 1995

4) Miller JP, Acar F, Hamilton BE, Burchiel KJ: Radiographic evaluation of trigeminal neurovascular compression in patients with and without trigeminal neuralgia. *J Neurosurg* 110: 627–632, 2009

5) Tanrikulu L, Scholz T, Nikoubashman O, Wiesmann M, Clusmann H: Preoperative MRI in neurovascular compression syndromes and its role for microsurgical considerations. *Clin Neurol Neurosurg* 129: 17–20, 2015

6) Devor M, Govrin-Lippmann R, Rappaport ZH: Mechanism of trigeminal neuralgia: an ultrastructural analysis of trigeminal root specimens obtained during microvascular decompression surgery. *J Neurosurg* 96: 532–543, 2002

7) Bazilevs Y, Hsu MC, Zhang Y, et al.: Computational vascular fluid-structure interaction: methodology and application to cerebral aneurysms. *Biomech Model Mechanobiol* 9: 481–498, 2010

8) Boussel L, Rayz V, McCulloch C, et al.: Aneurysm growth occurs at region of low wall shear stress: patient-specific correlation of hemodynamics and growth in a longitudinal study. *Stroke* 39: 2997–3002, 2008

9) Cebral JR, Vazquez M, Sforza DM, et al.: Analysis of hemodynamics and wall mechanics at sites of cerebral aneurysm rupture. *J Neurointerv Surg* 7: 530–536, 2015

10) Fukazawa K, Ishida F, Umeda Y, et al.: Using computational fluid dynamics analysis to characterize local hemodynamic features of middle cerebral artery aneurysm rupture points. *World Neurosurg* 83: 80–86, 2015

11) Hoi Y, Meng H, Woodward SH, et al.: Effects of arterial geometry on aneurysm growth: three-dimensional computational fluid dynamics study. *J Neurosurg* 101: 676–681, 2004

12) Meng H, Tutino VM, Xiang J, Siddiqui A: High WSS or low WSS? Complex interactions of hemodynamics with intracranial aneurysm initiation, growth, and rupture: toward a unifying hypothesis. *AJNR Am J Neuroradiol* 35: 1254–1262, 2014

13) Zhang Y, Jing L, Zhang Y, Liu J, Yang X: Low wall shear stress is associated with the rupture of intracranial aneurysm with known rupture point: case report and literature review. *BMC Neurol* 16: 231, 2016

14) Headache Classification Subcommittee of the International Headache Society: The International Classification of Headache Disorders: 2nd edition. *Cephalalgia* 24 Suppl 1: 9–160, 2004

15) Karmonik C, Diaz O, Klucznik R, et al.: Quantitative comparison of hemodynamic parameters from steady and transient CFD simulations in cerebral aneurysms with focus on the aneurysm ostium. *J Neurointerv Surg* 7: 367–372, 2015

16) Shojima M, Oshima M, Takagi K, et al.: Magnitude and role of wall shear stress on cerebral aneurysm: computational fluid dynamic study of 20 middle cerebral artery aneurysms. *Stroke* 35: 2500–2505, 2004

17) Takao H, Murayama Y, Otsuka S, et al.: Hemodynamic differences between unruptured and ruptured intracranial aneurysms during observation. *Stroke* 43: 1436–1439, 2012

18) Garcia M, Naraghi R, Zumbrunn T, Rösch J, Hastreiter P, Dörfler A: High-resolution 3D-constructive interference in steady-state MR imaging and 3D time-of-flight MR angiography in neurovascular compression: a comparison between 3T and 1.5T. *AJNR Am J Neuroradiol* 33: 1251–1256, 2012

19) Leal PR, Hermier M, Souza MA, Cristino-Filho G, Froment JC, Sindou M: Visualization of vascular compression of the trigeminal nerve with high-resolution 3T MRI: a prospective study comparing preoperative imaging analysis to surgical findings in 40 consecutive patients who underwent micro-vascular decompression for trigeminal neuralgia. *Neurosurgery* 69: 15–25; discussion 26, 2011

20) Antonini G, Di Pasquale A, Cruccu G, et al.: Magnetic resonance imaging contribution for diagnosing symptomatic neurovascular contact in classical trigeminal neuralgia: a blinded case-control study and meta-analysis. *Pain* 155: 1464–1471, 2014

21) Herweh C, Kress B, Rasche D, et al.: Loss of anisot-ropy in trigeminal neuralgia revealed by diffusion tensor imaging. *Neurology* 68: 776–778, 2007

22) Lin W, Zhu WP, Chen YL, et al.: Large-diameter compression arteries as a possible facilitating factor for trigeminal neuralgia: analysis of axial and radial diffusivity. *Acta Neurochir (Wien)* 158: 521–526, 2016

23) Malek AM, Alper SL, Izumo S: Hemodynamic shear stress and its role in atherosclerosis. *JAMA* 282: 2035–2042, 1999

24) Nixon AM, Gunel M, Sumpio BE: The critical role of hemodynamics in the development of cerebral vascular disease. *J Neurosurg* 112: 1240–1253, 2010

25) Kamath MV, Yamada Y, Kato Y: Computational fluid dynamics as an indicator of offending vessel in trigeminal neuralgia and hemifacial spasms. *Romanian Neurosurg* 32: 418–425, 2018

26) Satoh T, Yagi T, Onoda K, et al.: Hemodynamic features of offending vessels at neurovascular contact in patients with trigeminal neuralgia and hemifacial spasm. *J Neurosurg* 130: 1870–1876, 2019

27) Temkar P, Kato Y, Yamada Y, Ansari A: Is there a role for computational fluid dynamics (CFD) in neurovascular compression syndrome? *Romanian Neurosurg* 32: 290–296, 2018

Address reprint requests to: Kenji Yamada, MD, Department of Neurosurgery, Tokyo Medical and Dental University, 1-5-45 Yushima, Bunkyo-ku, Tokyo 113-8519, Japan.
e-mail: kyamada-tmd@umin.ac.jp